

Heat Transfer and Entropy Analysis for Mixed Convection in a Discretely Heated Porous Square Cavity

A. Maougal¹ and R. Bessaih²

Abstract: The present study is a numerical investigation of the irreversibility and heat transfer properties of a steady laminar mixed flow in a square cavity, filled with a saturated porous medium and heated by a discrete set of heat sources. The continuity, Navier-Stokes, energy and entropy generation equations have been solved by a finite volume method. Both heat transfer irreversibility and fluid friction irreversibility have been taken into account in the computations of entropy generation. Simulations have been carried out for Reynolds number $Re=20, 40, 80, 100, 200$, Darcy number, $Da=10^{-5}-10^{-1}$, Prandtl number, $Pr=0.015, 0.7, 10, 103$, and aspect ratio, $D/H=0.05, 0.10, 0.15, 0.2, 0.25$, expressly considering the influence of such parameters on the entropy generation and heat transfer processes. The effect of the irreversibility distribution function and aspect ratio has been also taken into account. The results are presented in terms of entropy generation, Nusselt and Bejan numbers. Finally, a general correlation between all these parameters is determined on the basis of the present findings.

Keywords: Mixed convection, Porous medium, Heat transfer, Entropy generation.

Nomenclature

Be	local Bejan number
\overline{Be}	average Bejan number
Br	Brinkman number
D	slot of inlet and outlet fluid flow, m
Da	Darcy number
D/H	aspect ratio

¹ Département de Physique, Université Mentouri-Constantine, Route de Ain El. Bey, 25000 Constantine, Algeria.

² Laboratoire LEAP, Département de Génie Mécanique, Université Mentouri-Constantine, Route de Ain El. Bey, 25000 Constantine, Algeria. Corresponding author: Bessaih.rachid@gmail.com, Phone/Fax: +213 31 81 88 63.

Ek	Eckert number
F	Forchheimer coefficient
Gr	Grashof number
g	gravitational acceleration, m/s ²
H	cavity height, m
K	permeability, m ²
k	thermal conductivity, W/m.K
Nu	local Nusselt number
\overline{Nu}	average Nusselt number
n	normal coordinate
Pr	Prandtl number
Re	Reynolds number
T	temperature, K
T ₀	ambient temperature, K
T _W	temperature of the hot wall, K
ΔT	temperature difference, K
S _{gen}	local entropy generation rate, W/m ³ .K
S _{gen}	dimensionless local entropy generation rate
S _t	dimensionless total entropy generation
U, V	dimensionless horizontal and vertical velocities in x- and y- directions, respectively
u,v	horizontal and vertical velocities in x- and y- directions, respectively, m/s
V	uniform inlet velocity, m/s
X, Y	dimensionless horizontal and vertical coordinates in X- and Y-directions, respectively
x, y	horizontal and vertical coordinates in x- and y-directions, respectively

Greek symbols

α	thermal diffusivity of the fluid, m ² /s
β	thermal expansion coefficient, K ⁻¹
ε	porosity
Θ	dimensionless temperature
λ	inertial coefficient
μ	dynamic viscosity, kg/m.s
ν	kinematic viscosity, m ² /s
ϕ	irreversibility distribution ratio
Φ	dimensionless viscous dissipation function
ψ	dimensionless stream function

Ω	dimensionless temperature difference
∇_x	gradient along x-coordinate
∇_y	gradient along y-coordinate

1 Introduction

Entropy generation, non-equilibrium thermodynamics, optimal transportation (Viliani, 2008), and sustainable development are terms increasingly used in recent decades by scientists. The need to get a maximum work with minimum effort while preserving the environment is probably the main aim of scientists and politicians. It is in this context that this work relies. In recent decades, many scientists working on different subjects are focusing of major interest to the second law of thermodynamics. Entropy has become a term used by biologists, mathematicians, sociologists, economists, architects, and especially by physicists.

Entropy is not only a principle of thermodynamics but also a life principle. The coming years will certainly experience a significant development of this subject. This has already begun by the Prigogine theorem (Prigogine and Kondepudi, 2002), Bejan constructal theory (Bejan and Lorente, 2006) and their different applications.

In this paper, the mixed convection flows in porous media within a square heated open cavity, the entropy generation and heat transfer are analyzed. Due to their wide applications in many areas of engineering systems development, the phenomenon of mixed convection in open cavities with heat transfer in porous media has received considerable attention. Practical applications of the studied configuration are diverse and have a significant impact in several areas such as: thermal insulation, cooling of electronic systems, geophysics, nuclear reactors, petroleum reservoirs, buildings, solar energy...etc.

In fact, there is a wide range of published works which covers these subjects. More precisely, transport phenomena in porous media (Ingham and Pop, 2005), convection in porous media (Nield and Bejan, 2006), Handbook of porous media (Vafai, 2005) and principles of heat transfer in porous media (Kaviany, 1999). Several experimental, analytical and numerical papers were published; such as (Shohel and Pop, 2006) numerically investigated a mixed convection in a square vented enclosure filled with a porous medium. Their study is based on the variation on the Péclet and Rayleigh numbers as well as the width of the fluid inlet. Their results showed that the width of the fluid inlet affects considerably the heat transfer and flow characteristics, for fixed values of the Péclet and Rayleigh numbers. Basak et al. (2010) numerically studied a mixed convection flows in a lid-driven square cavity with porous medium. The relevant parameters are Darcy number ($Da=10^{-5} - 10^{-3}$),

Grashof number ($Gr=10^3 - 10^5$), Prandtl number ($Pr=0.015 - 10$), and Reynolds number ($Re=1 - 10^2$). It has been noted that a significant result is that the average Nusselt numbers are almost invariant with Grashof number for $Pr=0.7$. Stiriba et al. (2010) investigated with a direct numerical simulation the flow structure and heat transfer characteristics, for a mixed convection past a three-dimensional open cubical cavity on a broad interval of Reynolds ($Re=10^2 - 10^3$) and Richardson (0.001–10) numbers. The study is on the interaction between the induced stream flow and the buoyancy flow from heated wall. The obtained results show that the Nusselt number increases slightly when the forced flow is dominating and when Reynolds and Grashof numbers are significantly important, natural convection comes into play and Nusselt number increases significantly. It can be noted that there are insufficient studies on mixed convection in porous media with entropy production, especially in open cavities; this was the main motivation that this work has been fulfilled.

The entropy production in porous media is essentially studied in many references such as (Baytas and Baytas, 2005), using Darcy's law and Boussinesq-incompressible approximation. Authors numerically resolved entropy production, momentum and energy equations for laminar natural convection with heat transfer in inclined saturated porous cavity. The parameters considered are the angle of inclination and the Darcy-Rayleigh number. They showed that they can determine the optimum angle by calculating the entropy production. In their paper, Makinde and Osalusi (2005), studied the entropy production for laminar flow through a channel filled with a porous medium. Their results show that heat transfer irreversibility dominates over fluid friction, and viscous dissipation has no effect on the entropy production rate at the centreline of the channel. The entropy generation in porous square cavities with four configurations of heat sources during laminar natural convection has been studied by Kaluri and Basak (2011), more fluids are considered ($Pr=0.0015, 0.7, 10, \text{ and } 1000$), $Da=10^{-6} - 10^{-3}$, $Ra=10^3 - 10^6$. Their results show that for different positions of heat sources, the flow characteristics are affected. Entropy generation increased with the increase of Da and the average Bejan number is less than 0.5. The importance of thermal boundary conditions of heated/cooled walls and their impact on the entropy production and heat transfer inside porous enclosure was studied by Zahmatkesh (2008). For $Ra=10 - 10^3$, the flow characteristics and the entropy generation were strongly influenced by the thermal boundary conditions (Zahmatkesh, 2008). Bensouici and Bessaïh (2010) numerically studied the mixed convection heat transfer in a vertical channel containing heat sources. Among their achievements, one can mention: the maximum temperature decreases with the Richardson number, while the Nusselt number increases. The same results are obtained when the matrix thickness is increased.

Other recent interesting contributions are the studies by Al-Ajmi and Mosaad (2012), Hamimid, Guellal, Amroune and Zeraibi (2012), Choukairy and Bennacer (2012) and Labeled, Bennamoun and Fohr (2012).

The present study is aimed to study the influence of the Reynolds number on the flow and thermal fields, on the average Bejan number, average Nusselt number and total entropy generation. The effects of Darcy number, Prandtl number, irreversibility distribution function and aspect ratio on the average Nusselt number, average Bejan number, and total entropy generation is also analyzed. Section 2 presents the mathematical formulation. Section 3 concerns the entropy generation analysis. Section 4 discusses the numerical method and techniques which have been used for the computation as well as the grid independence study and code validation. Section 5 presents the results and discussion, and finally a conclusion is given.

2 Governing equations

A two dimensional square vented cavity is filled with a fluid saturated porous medium. The porous medium is assumed to be homogeneous and isotropic. The configuration model and boundary conditions are shown in Fig.1. The Cartesian coordinate system is used in this problem. The left vertical wall is adiabatic and in the middle of the other walls are placed three discrete heat sources. The flow is modeled by the Darcy-Brinkman-Forchheimer equation in the porous matrix, and by the Navier–Stokes equations in the fluid domain. Mixed convection is due to the forced flow which enters from the bottom slot with a constant velocity V_0 and comes out through a slot at the upper border of the vertical surface. The thermo physical properties of the fluid and porous media are assumed to be constant (Kaluri and Basak, 2011).

The conservation equations of mass, momentum, and energy for a two-dimensional laminar mixed convection and steady incompressible flow with Boussinesq approximation were considered, using the following dimensionless variables:

$$X = \frac{x}{H}, \quad Y = \frac{y}{H}, \quad U = \frac{u}{V_0}, \quad V = \frac{v}{V_0}, \quad \Theta = \frac{T - T_0}{\Delta T}, \quad \Delta T = T_w - T_0, \quad \Omega = \frac{\Delta T}{T_0} \quad (1)$$

Continuity:

$$\frac{\partial U}{\partial X} + \frac{\partial V}{\partial Y} = 0 \quad (2)$$

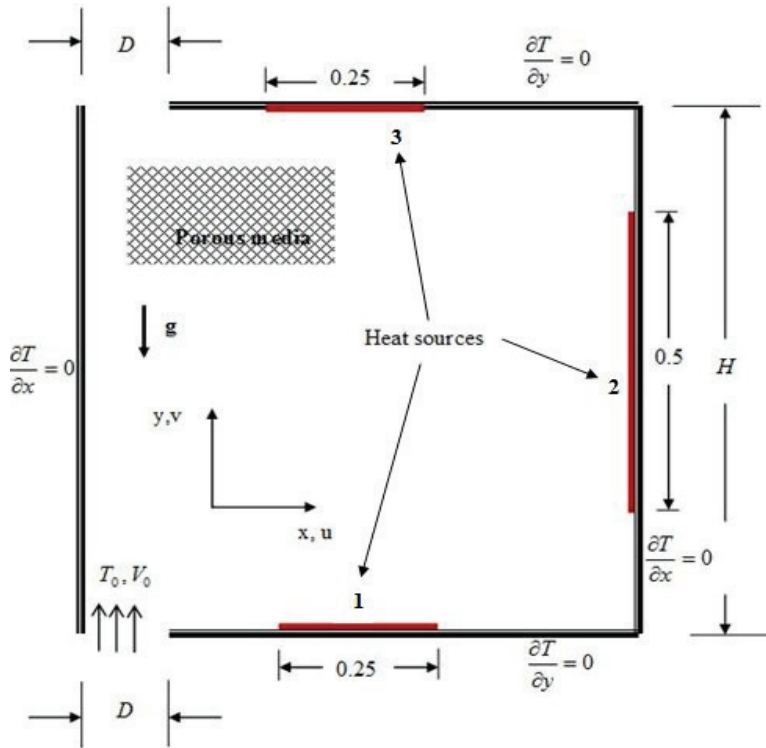


Figure 1: A square open cavity filled with a saturated porous medium. Three discretely heat sources are placed on the right, bottom and top walls.

X-momentum:

$$\frac{1}{\varepsilon^2} \left(U \frac{\partial U}{\partial X} + V \frac{\partial U}{\partial Y} \right) = -\frac{\partial P}{\partial X} + \frac{1}{\varepsilon Re} \left\{ \frac{\partial^2 U}{\partial X^2} + \frac{\partial^2 U}{\partial Y^2} \right\} - \frac{1}{Re Da} U - \lambda (U^2 + V^2)^{1/2} \cdot U \quad (3)$$

Y-momentum:

$$\frac{1}{\varepsilon^2} \left(U \frac{\partial V}{\partial X} + V \frac{\partial V}{\partial Y} \right) = -\frac{\partial P}{\partial Y} + \frac{1}{\varepsilon Re} \left\{ \frac{\partial^2 V}{\partial X^2} + \frac{\partial^2 V}{\partial Y^2} \right\} - \frac{1}{Re Da} V - \lambda (U^2 + V^2)^{1/2} \cdot V + \frac{Gr}{Re^2} \Theta \quad (4)$$

Energy:

$$U \frac{\partial \Theta}{\partial X} + V \frac{\partial \Theta}{\partial Y} = \frac{1}{Re Pr} \left\{ \frac{\partial^2 \Theta}{\partial X^2} + \frac{\partial^2 \Theta}{\partial Y^2} \right\} \quad (5)$$

where U and V are dimensionless velocity components in the X - and Y - directions, respectively, and λ represents the inertial coefficient ($\lambda = F/Da^{1/2}=0.35$ (Bensouici and Bessaïh, 2010)).

The Reynolds, Darcy, Grashof, and Prandtl numbers are defined, respectively, as follows:

$$Re = \frac{V_0 H}{\nu}, \quad Da = \frac{K}{H^2}, \quad Gr = \frac{g\beta (T_w - T_0) H^3}{\nu^2}, \quad Pr = \frac{\nu}{\alpha} \quad (6)$$

The dimensionless boundary conditions for our study are:

$$\text{At } X = 0, 0 \leq Y \leq 1 : U = 0, V = 0, \frac{\partial \Theta}{\partial X} = 0 \text{ (adiabatic wall)} \quad (7a)$$

$$\text{At } X = 1, 0.25 \leq Y \leq 0.75 : U = 0, V = 0, \Theta = 1 \text{ (heat source N}^\circ 2) \quad (7b)$$

$$\text{At } Y = 0, 0 \leq X \leq X/D : U = 0, V = 1, \Theta = 0 \text{ (inlet channel)} \quad (7c)$$

$$\text{At } Y = 0, 0.5 \leq X \leq 0.75 : U = 0, V = 0, \Theta = 1 \text{ (heat source N}^\circ 1) \quad (7d)$$

$$\text{At } Y = 1, 0.5 \leq X \leq 0.75 : U = 0, V = 0, \Theta = 1 \text{ (heat source N}^\circ 3) \quad (7e)$$

$$\text{At } Y = 1, 0 \leq X \leq X/D : \frac{\partial U}{\partial Y} = 0, \frac{\partial V}{\partial Y} = 0, \frac{\partial \Theta}{\partial Y} = 0 \text{ (outlet channel)} \quad (7f)$$

3 Entropy generation analysis

In this case, the entropy generation equation (Eq.8) includes three terms that quantify the irreversibility:

- A first term reflects the heat transfer.
- A second is related to the porous media.
- The last term corresponding to the viscous friction.

The local entropy generation (or the entropy generation number) is then (Bejan,1982):

$$s_{gen} = \frac{k}{T_0^2} \left[\left(\frac{\partial T}{\partial x} \right)^2 + \left(\frac{\partial T}{\partial y} \right)^2 \right] + \frac{\mu}{KT_0} (u^2 + v^2) + \frac{\mu}{T_0} \left\{ 2 \left[\left(\frac{\partial u}{\partial y} \right)^2 + \left(\frac{\partial v}{\partial x} \right)^2 \right] + \left(\frac{\partial u}{\partial y} + \frac{\partial v}{\partial x} \right)^2 \right\} \quad (8)$$

By using $k\Omega^2/H^2$, as typical scales for entropy generation, the dimensionless local entropy generation (Eq.8), which is called the entropy generation number, becomes (Bejan, 1982):

$$S_{gen} = \left[(\nabla_x \Theta)^2 + (\nabla_y \Theta)^2 \right] + \frac{Br}{\Omega Da} (U^2 + V^2) + \frac{Br}{\Omega} \Phi \quad (9)$$

∇_x and ∇_y are the gradients along the x and y coordinates, respectively. The term Br/Ω is generally translated by the irreversibility distribution ratio ϕ , which is defined as:

$$\phi = \frac{\text{Fluid - friction irreversibility}}{\text{Heat - transfer irreversibility}} \quad (10)$$

The dimensionless total entropy generation, S_t is obtained by integrating equation (9) as:

$$S_t = \int_V \left\{ [(\nabla_x \Theta)^2 + (\nabla_y \Theta)^2] + \frac{Br}{\Omega Da} (U^2 + V^2) + \frac{Br}{\Omega} \Phi \right\} dV \quad (11)$$

Heat transfer in the cavity is measured by the mean Nusselt number, which is equal to the dimensionless temperature (Sivasankaran et al., 2010):

$$\overline{Nu} = - \int_0^1 \left(\frac{\partial \Theta}{\partial Y} \right)_{Y=0} dX, \text{ for the bottom wall} \quad (12a)$$

$$\overline{Nu} = - \int_0^1 \left(\frac{\partial \Theta}{\partial X} \right)_{X=0} dY, \text{ for the left vertical wall} \quad (12b)$$

$$\overline{Nu} = - \int_0^1 \left(\frac{\partial \Theta}{\partial Y} \right)_{Y=1} dX, \text{ for the top wall} \quad (12c)$$

$$\overline{Nu} = - \int_0^1 \left(\frac{\partial \Theta}{\partial X} \right)_{X=1} dY, \text{ for the right vertical wall} \quad (12d)$$

In order to know the dominant irreversibility, it is necessary to introduce the local Bejan number Be that has the following expression:

$$Be = \frac{S_{gen,h}}{S_{gen,h} + S_{gen,f}} \quad (13)$$

where $S_{gen,h}$ and $S_{gen,f}$ are the local entropy generation due to heat transfer and fluid friction, respectively. When $Be > 0.5$ the heat transfer irreversibility dominates and when $Be < 0.5$ irreversibility is dominated by fluid friction effects (Bejan, 2006).

The average Bejan number \overline{Be} is found by integrating the local Bejan number as:

$$\overline{Be} = \frac{\int_A Be(X,Y).dA}{\int_A dA} \quad (14)$$

4 Numerical procedure

The governing equations (2-5), with the associated boundary conditions (7a-7f), were solved using a finite volume technique (Patankar, 1980). The components of the velocity (U and V) were stored at the staggered locations, and the scalar quantities (P and Θ) were stored in the centre of these volumes. A fully implicit scheme was employed. The numerical procedure called SIMPLER (Patankar, 1980) was used to handle the pressure-velocity coupling. For treatment of the convection and diffusion terms in equations (2-5), central difference scheme was adopted. Finally, the discretized algebraic equations were solved by the line-by-line tri-diagonal matrix algorithm (TDMA). Convergence was obtained when the maximum relative change between two consecutive iteration levels is defined as:

$$\left| \frac{\Lambda_{i,j}^{n+1} - \Lambda_{i,j}^n}{\Lambda_{i,j}^{n+1}} \right| < 10^{-5} \quad (15)$$

where Λ denotes one of the main variables U, V, Θ and n is the iteration index. Calculations were carried out on a PC (Intel Core 2 Duo) with 2.00 GHz CPU.

4.1 Grid independence study

Different mesh sizes were chosen to find the appropriate grid. A regular grid is used and increasing the mesh size from 82×82 to 222×222 nodes. Due to the relative error on the entropy generation which is rather small, the mesh size 202×202 nodes, has therefore been chosen. The relative error is defined as follows:

$$Error \% = \left| \frac{N_{s(k,k)}^2 - N_{s(k,k)}^1}{N_{s(k,k)}^1} \right| \quad (16)$$

where $N_{s(k,k)}$ is the previously calculated value of the entropy generation rate corresponding to the mesh size (k, k). Table 1 represents the different values of entropy generation rate for each chosen grid and the associated relative error. This calculation is done for the fixed thermal convective parameters: $Gr=10^4$, $Re=100$, $Pr=0.71$, $\varepsilon=1$, $Da=10^{-3}$, $D/H=0.25$ and $\phi=10^{-2}$.

4.2 Code validation

The numerical code was validated with the numerical results of Megherbi et al. (2003). Essentially, their study is based on the Rayleigh number effect on the entropy generation and the irreversibility distribution ratio. As shown in Fig. 2, it is clear that the present work is in a good agreement with the numerical results of Megherbi et al. (2003).

Table 1: Results of the grid independence tests, for $Gr=10^4$, $Re=100$ ($Ri=1$), $Da=10^{-3}$, $Pr=0.71$ (air), $\phi=10^{-2}$, $D/H=0.25$.

Grid	Total entropy generation
82×82 nodes	7.300
142×142 nodes	7.530
182×182 nodes	7.604
202×202 nodes	7.632
222×222 nodes	7.657

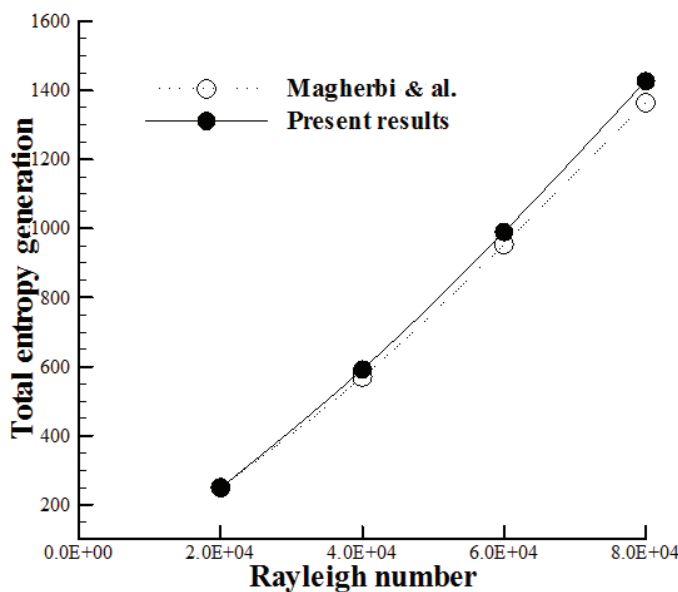


Figure 2: Variation of the dimensionless total entropy generation versus Rayleigh number ($Ra= 2 \times 10^4$, 4×10^4 , 6×10^4 , and 8×10^4): Comparison between the present results and those of Megherbi et al. (2003).

5 Results and discussion

This work is devoted to study the effect of some thermo-convective parameters on heat transfer and entropy generation. The interest has especially given to determine the parameters giving the maximum heat transfer and the lowest entropy generation. The value of the Grashof number Gr is equal to 10^4 in all the numerical simulations. The adopted ranges are: Reynolds number, $Re=20, 40, 80, 100, 200$, Darcy number, $Da=10^{-5}-10^{-1}$, Prandtl number, $Pr=0.015, 0.7, 10, 10^3$ and aspect ratio $D/H=0.05$,

0.10, 0.15, 0.2, 0.25. It can be noted that for $Gr=10^4$, the values of Reynolds numbers ($Re=200, 100, 80, 40, 20$) correspond to the values of Richardson numbers ($Ri= 0.25, 1, 1.5625, 6.250, 25$), respectively. All these results are presented in dimensionless values.

5.1 Effect of Reynolds number

In order to make a wide investigation, three Richardson number values are considered: $Ri < 1$, $Ri = 1$ and $Ri > 1$. Dimensionless stream function (defined as: $U = \partial\psi/\partial Y$) and dimensionless temperature Θ are plotted in Fig3 with fixing the following parameters: $Gr=10^4$, $Pr=0.71$, $\varepsilon=1$, $Da=10^{-3}$, $D/H=0.25$, $\phi=10^{-2}$.

When $Ri > 1$, the $Ri=6.25$ case is taken which is equivalent to $Re=40$, this represents a low-speed flow, so the natural convection dominates. When the Richardson number decreases, forced convection becomes more important and the isothermal contour plots are pushed around the heat sources. Fig 4a shows that the local Bejan number is greater than 0.5, which proves that the heat transfer irreversibility dominates the fluid friction irreversibility. This explains the similarity between dimensionless total entropy generation rate and average Nusselt number variations in Fig 4b. The increase in Reynolds number promotes heat transfer and increases the irreversibility, as has been demonstrated by (Khan et al., 2006 and Eiyad Abu-Nada, 2006).

To get an idea about the spatial distribution of entropy generation, Fig.5 illustrates a three dimensional view of the total entropy generation, S_t . According to this figure, it can be shown that friction is significant at the entrance and exit of the flow. The latter is translated by the fluid friction irreversibility but not as important as the heat transfer irreversibility which is displayed by the peaks on the heat sources. It may also be noted that the heat transfer irreversibility is more important than the fluid friction irreversibility.

For the Reynolds number values varying from 20 to 200 at $Pr=0.71$, $Da=10^{-3}$, $Gr=10^4$ ($Ri=1$), $\varepsilon=1$, $D/H=0.25$, the total entropy generation S_t , average Nusselt number \overline{Nu} , and average Bejan number \overline{Be} can be correlated by the following equations, respectively as:

$$S_t = 1.3108Re^{0.3788} \quad (17a)$$

$$\overline{Nu} = 1.0519Re^{0.4538} \quad (17b)$$

$$\overline{Be} = 2.7938Re^{0.1601} \quad (17c)$$

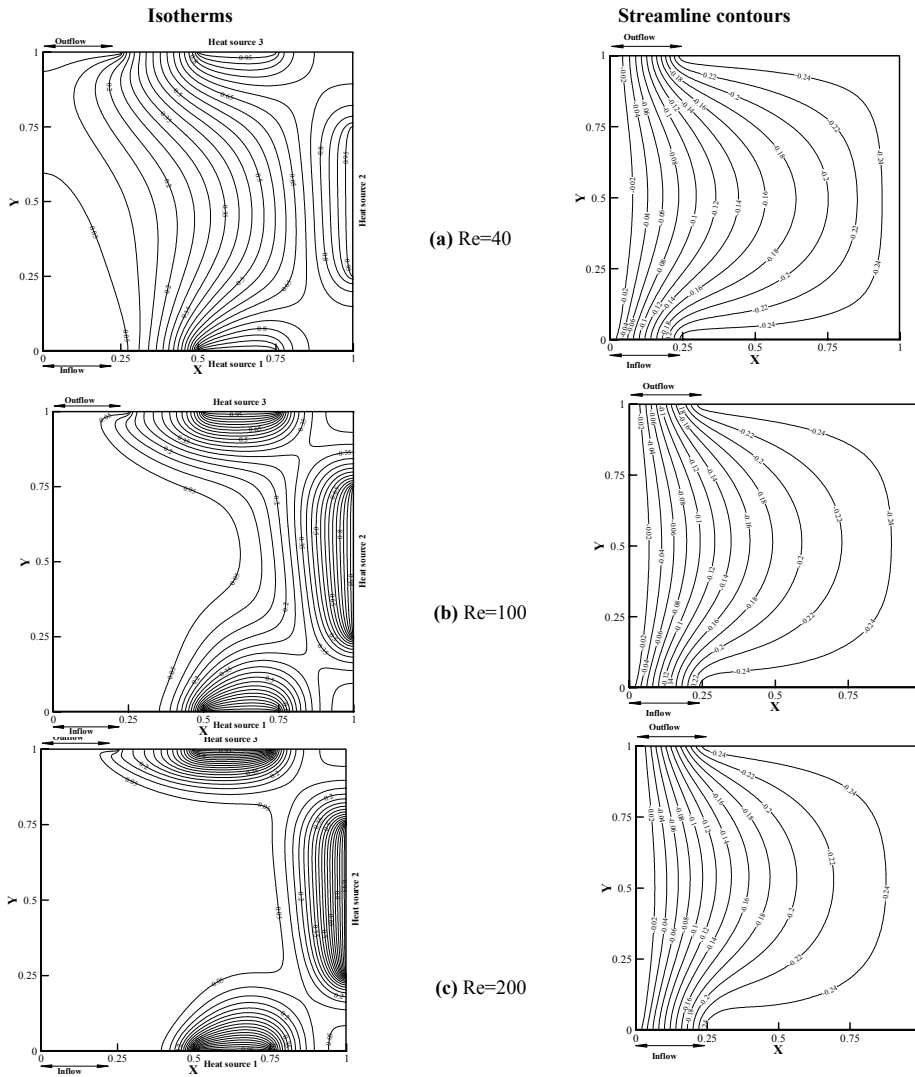
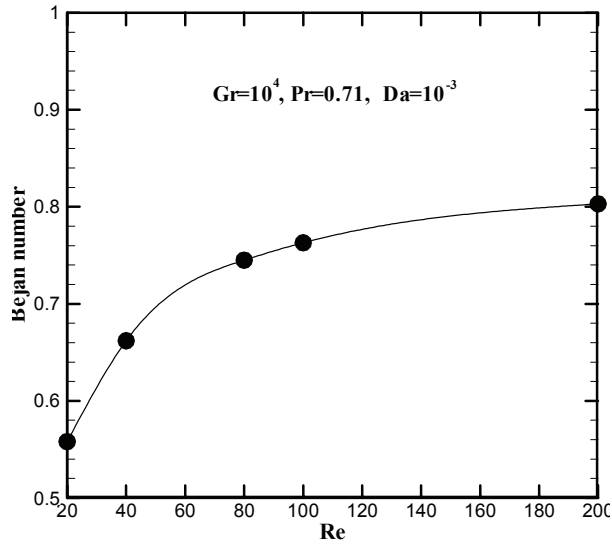
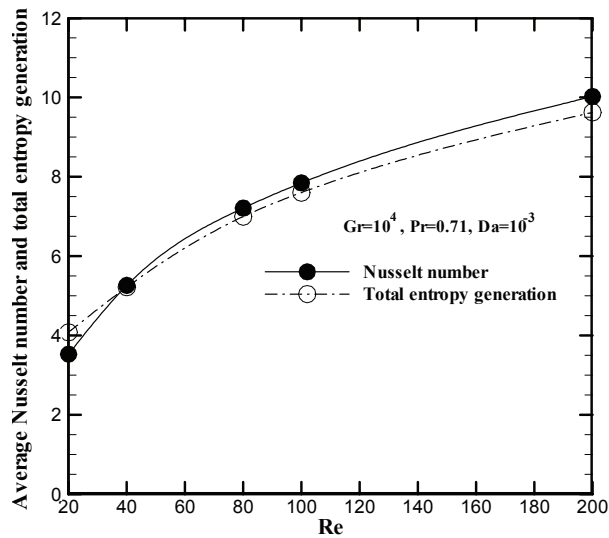


Figure 3: Streamline contours ψ (on the right) and isotherms Θ (on the left) at $Gr=10^4$, $Da=10^{-3}$, $Pr=0.71$ (air), $\phi=10^{-2}$, $D/H=0.25$, and for various values of the Reynolds number (a) $Re=40$, (b) $Re=100$, and (c) $Re=200$, which correspond to the values of the Richardson number, $Ri=Gr/Re^2=6.250$, 1 , and 0.25 , respectively.



(a)



(b)

Figure 4: Effect of the Reynolds number Re ($=20, 40, 80, 100$, and 200) on (a) average Bejan number and (b) average Nusselt number and total entropy generation, for $Gr=10^4$, $Da=10^{-3}$, $Pr=0.71$ (air), $\phi=10^{-2}$, and $D/H=0.25$.

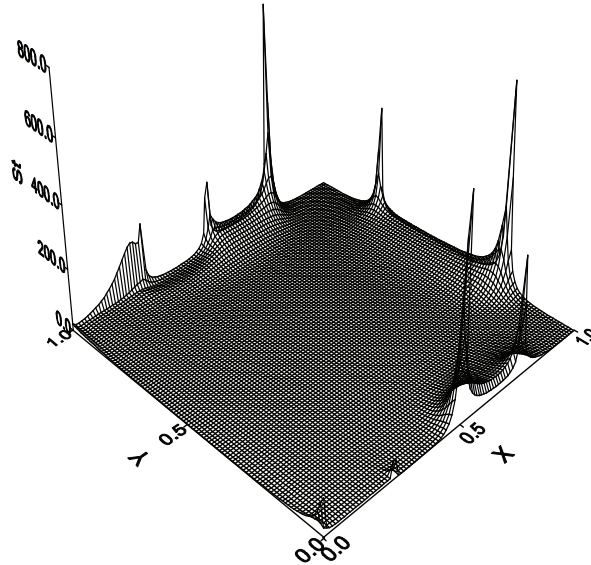


Figure 5: Total entropy generation variation St for $Gr=10^4$, $Re=200$ ($Ri =0.25$), $Da=10^{-3}$, $Pr=0.71$ (air), $\phi=10^{-2}$, and $D/H =0.25$.

5.2 Effect of Darcy number

The fixed parameters are: $Gr=10^4$, $Re=100$ ($Ri=1$), $Pr=0.71$, $\varepsilon=1$, $D/H=0.25$. Darcy number is the porous medium dimensionless permeability. It reflects the fluids flow conductance through the porous medium. Its increase promotes better convection. This would lead to a better convective heat transfer. Fig.6a shows that the average Nusselt number decreases as the Darcy number increases, this means that the heat transfer is largely done by conduction and heat diffusion more than heat convection in the porous region (Vafai and Huang, 1994), the extreme case has been dealt with, where the porosity is equal to one. The average Bejan number increases with Darcy number (Fig.6b). Bejan number shows the dominant irreversibility, which can be expressed in terms of the irreversibility distribution ratio by:

$$Be = \frac{1}{1 + \phi} \quad (18)$$

For the Darcy number value, $Da=10^{-5}$, $Be \rightarrow 0$, which is equivalent to ϕ tend to infinity, from the ϕ definition in equation (10) the fluid-friction irreversibility dominates. $Be \rightarrow 1$ is the opposite limit at which the heat transfer irreversibility dominates and which corresponds to $Da=10^{-1}$. Physically, it is acceptable then the heat transfer increases with permeability (Nield and Bejan, 2006) The Darcy number

effect on the entropy generation is depicted in Fig.6c, which shows that entropy production decreases when Da decreases. Entropy generation is related to irreversible processes. In this case it is about of thermal transfer and fluid friction processes. When Da increases, the frictional resistance is less important in the porous medium. Fig.6c shows that heat transfer is mainly controlled by diffusion, which causes a decrease in entropy generation. The porous medium is the main cause of this irreversibility. It can be concluded that the Entropy Generation Minimization (EGM) principle is not verified in this case and the heat transfer decreases with entropy production. Table 2 represents the heat transfer and total entropy generation values for two cases: with and without the porous medium, the introduction of the porous medium increases the heat transfer and reduces the total entropy generation, which is in agreement with the EGM principle.

Table 2: Average Nusselt number, total entropy generation and average Bejan number with and without porous medium.

	Average Nusselt number	Total entropy generation	Average Bejan number
With porous ($Da=10^{-3}$)	7.854	7.632	0.763
Without porous	7.687	8.015	0.717

For the Darcy number values ($10^{-5} < Da < 10^{-1}$) at $Gr=10^4$, $Re=100$ ($Ri=1$), $Pr=0.71$, $\varepsilon=1$, and $D/H=0.25$, the total entropy generation S_t , average Nusselt number \overline{Nu} , and average Bejan number \overline{Be} can be correlated, respectively, as:

$$S_t = \frac{1.5872}{Da^{0.3289}} \quad (19a)$$

$$\overline{Nu} = \frac{7.5594}{Da^{0.0058}} \quad (19b)$$

$$\overline{Be} = 3.5687Da^{0.3239} \quad (19c)$$

5.3 Effect of Prandtl number

It characterizes the relative importance of viscous and thermal effects. For fluids of high Prandtl number, thermal time is larger than the viscous time and heat process diffusion drive the fluid motion. For small values of Prandtl number, thermal effects are dwindling and the fluid behavior is essentially hydrodynamic. To achieve a wide investigation, four different fluids have been considered: $Pr=0.015$ (Liquid metal), $Pr=0.71$ (air), $Pr=10$ (Aqueous solutions), $Pr=1000$ (Engine Oils). Several works such as (Rahman et al., 2011) show that the Nusselt number and entropy generation

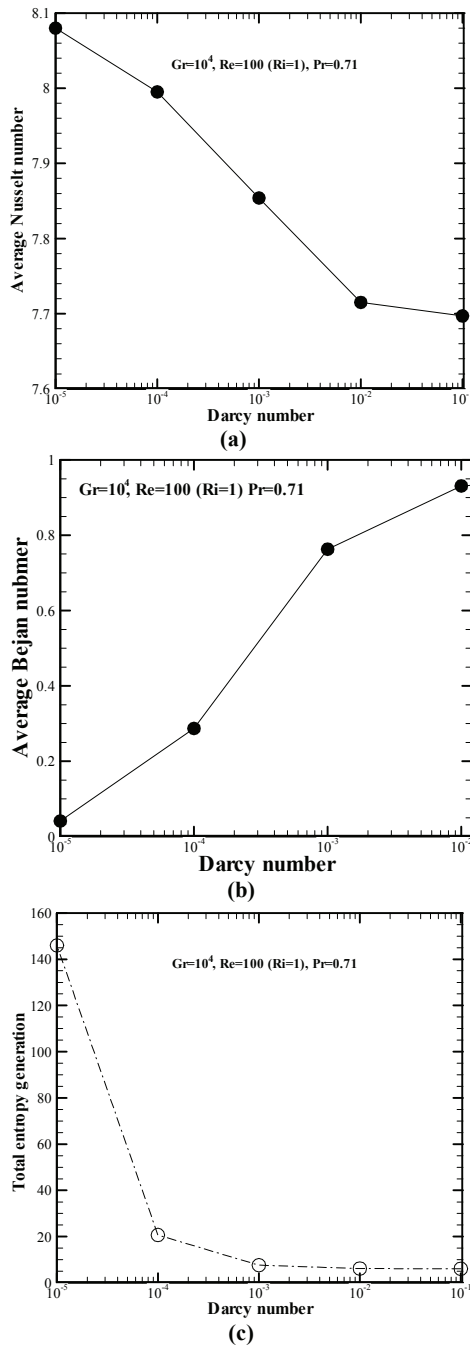


Figure 6: Effect of Darcy number Da ($=10^{-5}$, 10^{-4} , 10^{-3} , 10^{-2} , and 10^{-1}) on (a) average Nusselt number (b) average Bejan number and (c) total entropy generation, for $Gr=10^4$, $Re=100$ ($Ri=1$), $Da=10^{-3}$, $Pr=0.71$ (air), $\phi=10^{-2}$, and $D/H=0.25$.

increases with Prandtl number. Fig.7 shows the local heat entropy generation which clearly increases with the Prandtl number. The Bejan number can be interpreted as the ratio of viscous forces on heat transfer (Bejan et al., 2003).

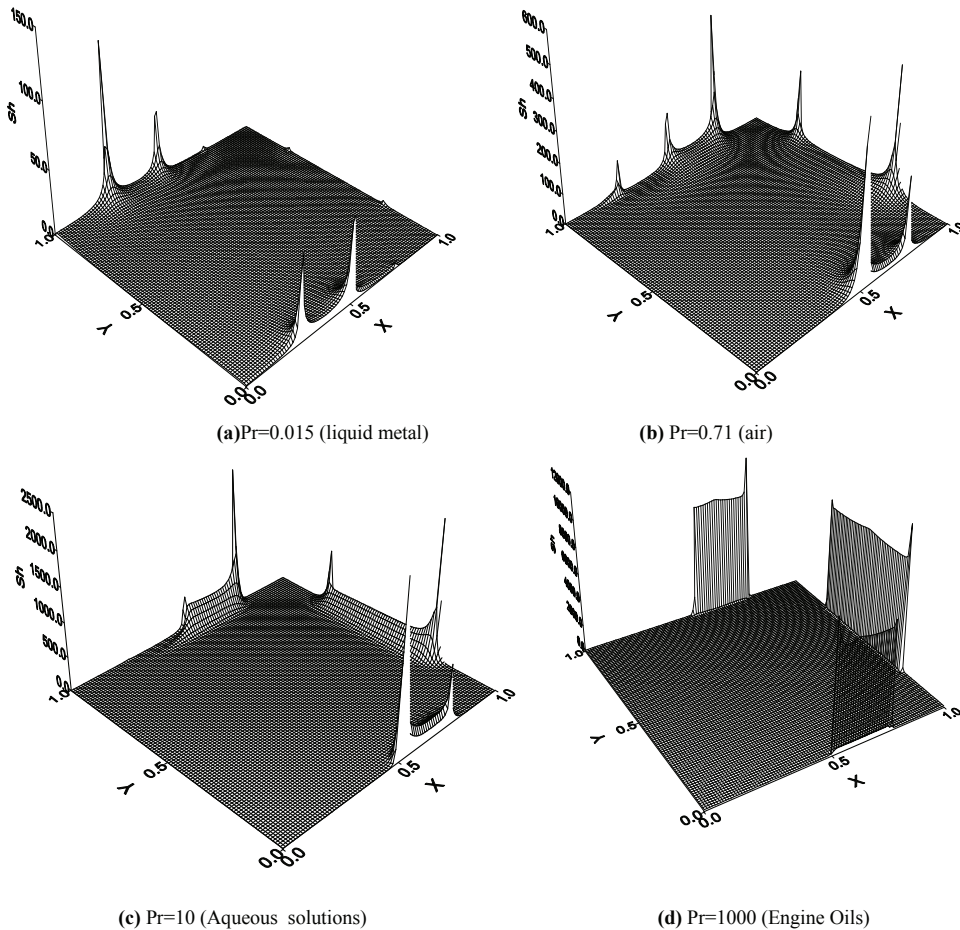


Figure 7: Local heat entropy generation variation in the X-Y plane, for various Prandtl numbers ($Pr=0.015, 0.71, 10,$ and 1000) at $Gr=10^4, Re=100$ ($Ri=1$), $Da=10^{-3}$, $\phi=10^{-2}$, and $D/H =0.25$.

Figure 8 shows the distribution of local Bejan number in the cavity. By increasing the Prandtl number or the fluid viscosity, viscous forces become more important and have an effect on thermal diffusion. The local Bejan number indicates that the heat transfer irreversibility concentrates near heat sources. Increasing Prandtl

number has an effect on the heat diffusion, which generates an increase on the Nusselt, Bejan numbers and entropy generation (figures 9a and 9b). The work results are confirmed by those found by Tamayol et al. (2010).

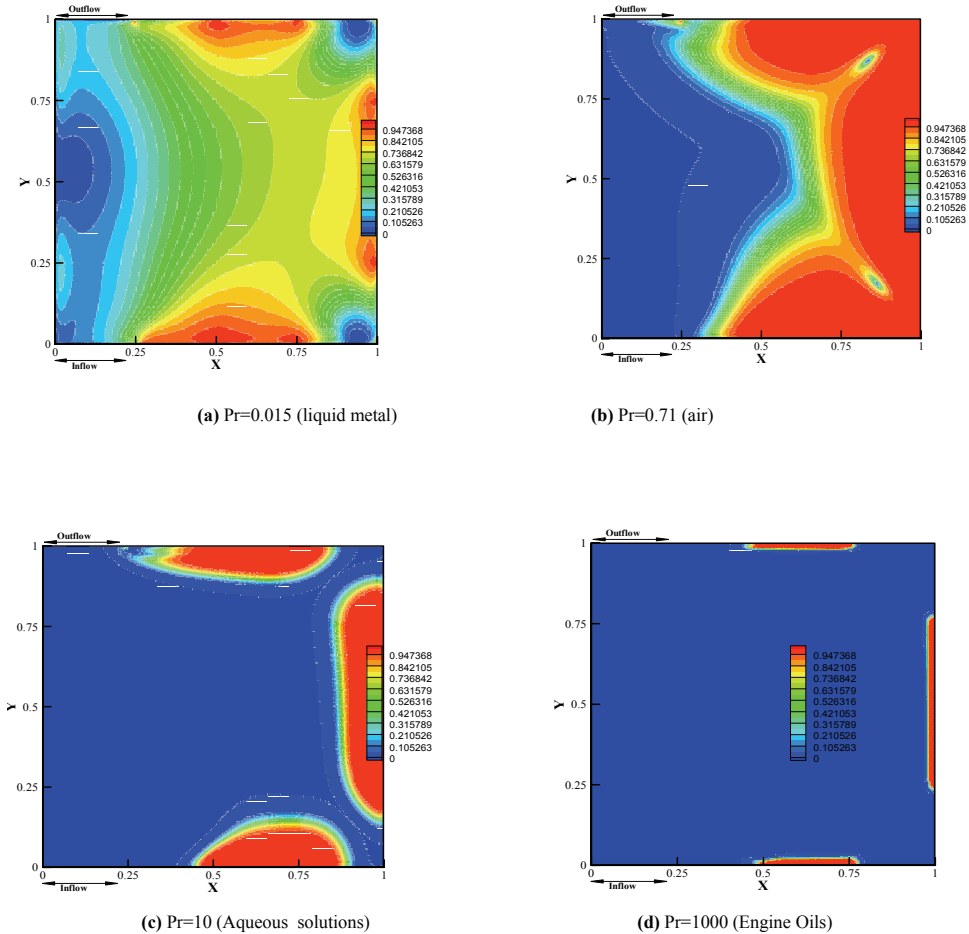


Figure 8: Local Bejan number variation in the X-Y plane, for various Prandtl numbers ($Pr=0.015, 0.71, 10, \text{ and } 1000$) at $Gr=10^4, Re=100$ ($Ri=1$), $Da=10^{-3}$, $\phi=10^{-2}$, and $D/H=0.2$

For the Prandtl number values (0.0015, 0.71, 10, 1000) at $Da=10^{-3}$, $Gr=10^4$, $Re=100$ ($Ri=1$), $\varepsilon=1$, $D/H=0.25$, the total entropy generation S_t , Nusselt average number

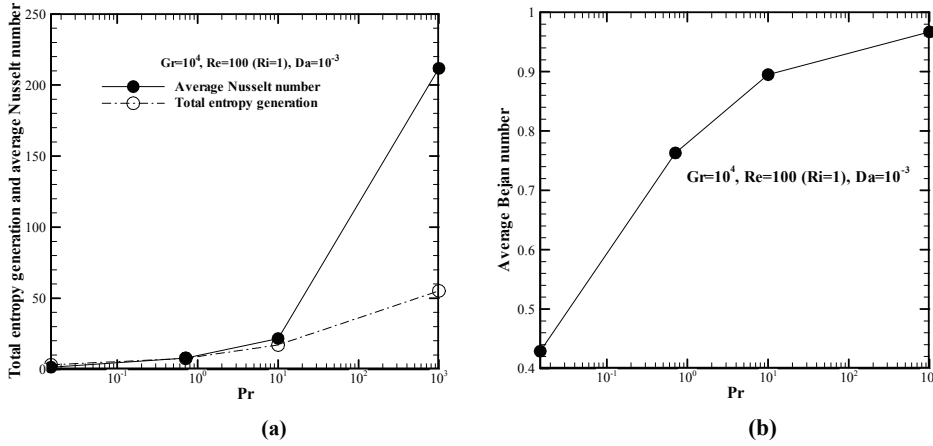


Figure 9: Effect of Prandtl number Pr ($=0.015, 0.71, 10$, and 1000) on (a) total entropy generation and average Nusselt number and (b) average Bejan number, for $Gr=10^4$, $Re=100$ ($Ri=1$), $Da=10^{-3}$, $\phi=10^{-2}$, and $D/H=0.25$.

\overline{Nu} , and Bejan average number \overline{Be} can be correlated, respectively as follows:

$$S_t = 9.0494Pr^{0.2606} \quad (20a)$$

$$\overline{Nu} = 9.0178Pr^{0.4449} \quad (20b)$$

$$\overline{Be} = 1.4889Pr^{0.0709} \quad (20c)$$

Vertical and horizontal velocity profiles along the lines $Y=0.5$ and $X=0.5$ are presented in Fig.10, for $Gr=10^4$, $Ri=1.0$ and $Pr=0.71$. The two transversal velocities have the same appearance except in the case with porous medium, the velocity has a negative minimum to the abscissa $X=0.7$. The velocity vertical component is more intense in the presence of the porous medium, which implies that the porous medium promotes the transport of kinetic energy. The axial velocity profile is complex as a result of the interaction between the mixed convection with energy inside and the buoyancy forces. There is a braking effect by the porous medium which promotes heat transfer.

5.4 Effect of irreversibility distribution ratio

Variation of total entropy generation according to ϕ is depicted in Fig.11; the irreversibility distribution ratio is defined as the ratio between the fluid friction irreversibility and the heat transfer irreversibility and gives an idea of the dominant irreversibility. This is the case where $0 \leq \phi < 1$, which implies that the heat transfer

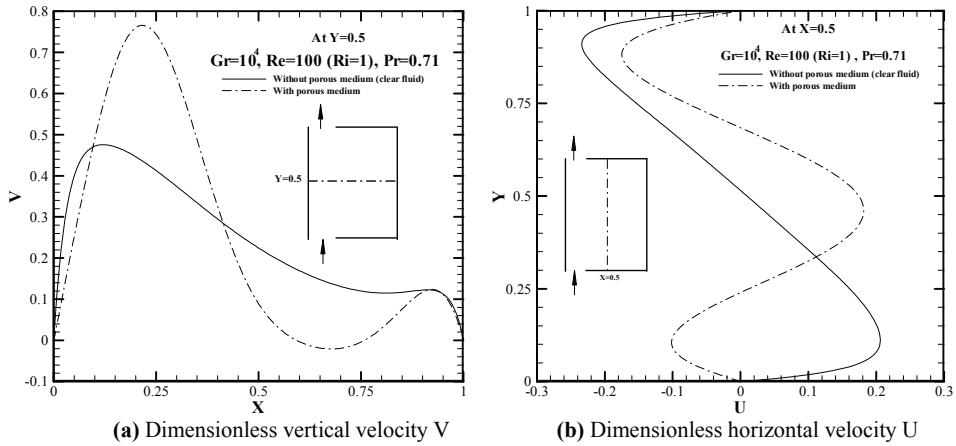


Figure 10: Variation of (a) horizontal velocity U at $Y=0.5$ and (b) vertical velocity V at $X=0.5$, with and without porous medium (clear fluid), for $Gr=10^4$, $Re=100$ ($Ri=1$), $Pr=0.71$ ($Ri=1$), $Pr=0.71$, and $D/H = 0.25$.

irreversibility is dominant. Increasing the irreversibility distribution ratio, the total entropy generation increases. In considering the ϕ definition, this result may be explained. The latter can be expressed as $\frac{Br}{\Omega}$, where Br is the Brinkman number which is equal to the $Pr \cdot Ek$ product. As already shown, the entropy production increases with Prandtl number. Eckert number expresses the relationship between a flow's kinetic energy and enthalpy. When the kinetic energy increases, the flow becomes more intense which has the effect of increasing the entropy production. The enthalpy is related to the temperature difference ΔT ; it is the denominator as defined Ek , heat transfer becomes more important by its increase and finally the entropy production increases. Same results were obtained by Hooman and Ejlali (2007).

5.5 Effect of the aspect ratio

Figure 12 is an answer to the question: is there an optimal aspect ratio? The principle EGM stipulates that the maximum power output corresponds to the minimum entropy generation (Bejan, 2009). The total entropy generation is plotted according to the aspect ratio D/H and 0.2 is a maximum value of D/H , what does this mean? It is important to note that the physical system geometry has an effect on the entropy production as already announced, it is hoped to find a minimum entropy production in order to optimize the physical system by applying the EGM principle, but the opposite was found. It is known that the relationship between the minimum en-

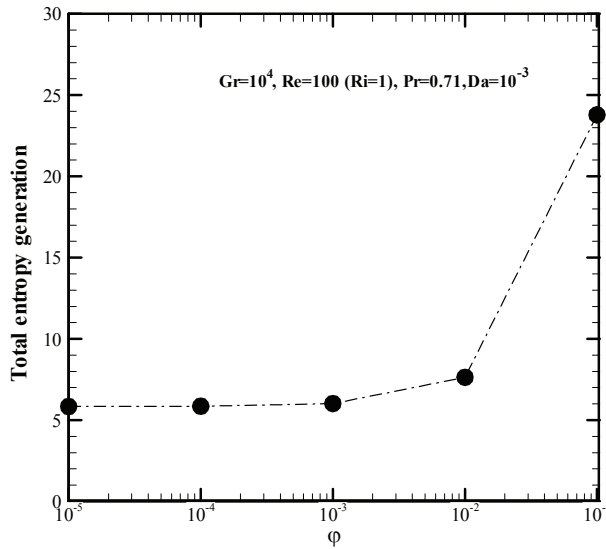


Figure 11: Effect of the irreversibility distribution ratio ϕ ($=10^{-5}$, 10^{-4} , 10^{-3} , 10^{-2} , and 10^{-1}) on the total entropy generation for $Gr=10^4$, $Re=100$ ($Ri=1$), $Pr=0.71$, $Da=10^{-3}$, and $D/H=0.25$.

ropy production principle and maximum entropy production principle is not simple (Martyushev and Seleznev, 2006). It has been shown for an open system evolving toward a steady state, there is a thermodynamic path that maximizes its entropy production. Furthermore, it was confirmed that the principle of maximizing the entropy production for irreversible open systems is a theoretical investigation that aims to analyze their stability. This is confirmed by the same author: "a steady state is stable if the entropy generation is maximum" (Lucia, 2012). According to the previously mentioned, the value of the aspect ratio that corresponds to the value 0.2 is a value for which the entropy production is at its maximum, it implies that the physical system reaches a steady and stable state. It can also be noticed that the heat transfer depends on the geometry of the physical system in question and the same value of the aspect ratio ($D/H=0.2$) performs better from the heat transfer point of view.

6 Conclusions

This study was focused on the influence of mixed convection intensity, porous media compactness and fluid nature on the heat transfer and irreversibility. The parameters having an effect on the problem are: Reynolds number Re , Darcy number

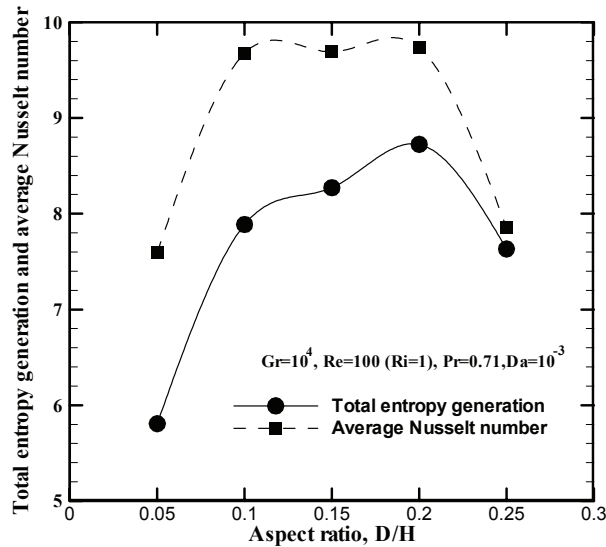


Figure 12: Effect of aspect ratio D/H ($=0.05, 0.1, 0.15, 0.2,$ and 0.25) on the total entropy generation and average Nusselt number for $Gr=10^4$, $Re=100$ ($Ri=1$), $Pr=0.71$, $Da=10^{-3}$, $\phi=10^{-2}$.

Da , Prandtl number Pr , irreversibility distribution ratio ϕ , and aspect ratio D/H . The Grashof number is considered constant, $Gr=10^4$. The heat transfer is improved by increasing the Reynolds and Prandtl numbers. They have the same effect on the entropy production. It is interesting to note that it has a profitable effect when the porous medium is introduced into the cavity in the sense where a better heat transfer and lowest entropy production are obtained. This is in agreement with EGM principle. Entropy generation rate, Bejan number and heat transfer increases with Da . Re and Pr have the same effect on the Bejan number and the entropy generation rate increases with the irreversibility distribution ratio. There is an aspect ratio for which the entropy generation and heat transfer are maximum, it can be concluded that the physical system must be stable for this value and the EGM principle is not applicable for this case.

References

- Al-Ajmi, R.; Mosaad, M.** (2012): Heat Exchange between Film Condensation and Porous Natural Convection across a Vertical Wall. *Fluid Dynamics & Materials Processing*, vol. 8, No. 1, pp. 51-68.
- Basak, T.; Roy, S.; Singh, S.K.; Pop, I.** (2010): Analysis of mixed convection

in a lid-driven porous square cavity with linearly heated side walls. *International Journal of Heat and Mass Transfer*, vol. 53, pp. 1819–1840.

Baytas, A.C.; Baytas, A.R. (2005): *Entropy Generation in Porous Media*, Chapter 8 of *Transport Phenomena in Porous Media*, Elsevier, First edition

Bejan, A.; Lorente, S. (2006): Constructal theory of generation of configuration in nature and

engineering. *Journal of Applied Physics*, vol. 100, no. 041301.

Bejan, A. (1982): *Entropy Generation Through Heat and Fluid Flow*, Willey & Sons.

Bejan, A. (2006): *Advanced Engineering Thermodynamics*, 3rd Edition, Willey & Sons.

Bejan, A.; Boyett, J.H.; Kraus, A.D. (2003): *Heat Transfer Handbook*, Wiley-Inter-science.

Bejan, A. (2009): Science and technology as evolving flow architectures. *International Journal of Energy Research*, vol. 33, pp. 112–125.

Bensouici, M.; Bessaih, R. (2010): Mixed convection in a vertical channel with discrete heat sources using a porous matrix. *Numerical Heat Transfer, Part A*, vol. 58, pp. 581–604.

Choukairy, K.; Bennacer, R. (2012): Numerical and Analytical Analysis of the Thermosolutal Convection in an Heterogeneous Porous Cavity. *Fluid Dynamics & Materials Processing*, vol. 8, no. 2, pp. 155-173.

Eiyad Abu-Nada. (2006): Entropy generation due to heat and fluid flow in backward facing step flow with various expansion ratio. *International Journal of Exergy*, vol. 3, pp. 419–435.

Hamimid, S., Guellal, M., Amroune, A.; Zeraibi N. (2012): Effect of a Porous Layer on the Flow Structure and Heat Transfer in a Square Cavity. *Fluid Dynamics & Materials Processing*, vol. 8, no. 1, pp. 69-90.

Hooman, K.; Ejlali, A. (2007): Entropy generation for forced convection in a porous saturated circular tube with uniform wall temperature. *International Communications in Heat and Mass Transfer*, vol. 34, pp. 408–419.

Ingham, D.B.; Pop, I. (2005): *Transport Phenomena in Porous Media*, Elsevier, Oxford.

Kaluri, R.S.; Basak, T. (2011): Role of entropy generation on thermal management during natural convection in porous square cavities with distributed heat sources. *Chemical Engineering Science*. vol. 66, pp. 2124–2140.

Kaviany, M. (1999): *Principles of Heat Transfer in Porous Media*, Springer.

Khan, W.A.; Culham, J.R.; Yonovich, M.M. (2006): The role of fin geometry in heat sink performance. *ASME Journal of Electronic Packaging*, vol. 128, pp. 324–329.

Labed, N.; Bennamoun, L.; and Fohr, J.P. (2012): Experimental Study of Two-Phase Flow in Porous Media with Measurement of Relative Permeability. *Fluid Dynamics & Materials Processing*, vol. 8, no. 4, pp. 423-436.

Lucia, U. (2012): Maximum or minimum entropy generation for open systems? *Physica A*, vol. 391, pp. 3392–3398.

Magherbi, M.; Abbassi, H.; BenBrahim, A. (2003): Entropy generation at the onset of natural convection. *International Journal of Heat and Mass Transfer*, vol. 46, pp. 3441–3450.

Makinde, O.D.; Osalusi, E. (2005): Second law analysis of laminar flow in a channel filled with saturated porous media. *Entropy Journal*, vol. 7, pp. 148–160.

Martyushev, L.M.; Seleznev, V.D. (2006): Maximum entropy production in physics. *Chemistry and Biology*, Physics reports, vol. 426, pp.1–45.

Nield, D.A.; Bejan, A. (2006): *Convection in Porous Media*, Springer.

Patankar, S.V. (1980): *Numerical Heat Transfer and Fluid Flow*. McGraw-Hill, New York.

Prigogine, I.; Kondepudi, D. (2002): *Modern Thermodynamics from Heat Engines to Dissipative Structures*, Wiley & Sons.

Rahman, M.M.; Öztop, H.F.; Rahim, N.A.; Saidur, R.; Khaled Al-Salem. (2011): Reynolds and Prandtl numbers effects on MHD mixed convection in a lid-driven cavity along with Joule heating and a centered heat conducting circular block. *International Journal of Mechanics Materials Engineering*, vol. 5, pp. 163–170.

Shohel, M. Pop, I. (2006): Mixed convection in a square vented enclosure filled with a porous media. *International Journal of Heat and Mass Transfer*, vol. 49, pp. 2190–2206.

Sivasankaran, K.; Seetharamu, K.N.; Natarajan, R. (2010): Numerical study on mixed convection in a lid-driven cavity with non uniform heating on both sidewalls. *International Journal of Heat and Mass Transfer*, vol. 53, pp. 4304–4315.

Stiriba, Y.; Grau, F.X.; Ferré, J.A.; Vernet, A. (2010): A numerical study of three-dimensional laminar mixed convection past an open cavity. *International Journal of Heat and Mass Transfer*, vol. 53, pp. 4797–4808.

Tamayol, A.; Hooman, K.; Bahrami, M. (2010): Thermal analysis of flow in a porous medium over a permeable stretching wall *Transport in Porous Media*, vol. 85, pp. 661–676.

- Vafai, K.** (2005): *Principles of Heat Transfer in Porous Media*, CRC Press.
- Vafai, K.; Huang, C.** (1994): Analysis of heat transfer regulation and modification employing intermittently emplaced porous cavities. *ASME Journal of Heat Transfer*, vol. 116, pp.604–613.
- Villani, C.** (2008): *Optimal Transport: Old and New*, Springer.
- Zahmatkesh, I.** (2008): On the importance of thermal boundary conditions in heat transfer and entropy generation for natural convection inside a porous enclosure. *International Journal of Thermal Sciences* vol.47, pp. 339–346.

